DEUTSCHES ELEKTRONEN-SYNCHROTRON DESY

DESY 75/08
April 1975

The Bethe Salpeter Equation and the Relativistic Quark Model

by

Tamara S. Eisenschitz

2 HAMBURG 52 · NOTKESTIEG 1

To be sure that your preprints are promptly included in the
HIGH ENERGY PHYSICS INDEX ,
send them to the following address (if possible by air mail) :

DESY
Bibliothek
2 Hamburg 52
Notkestieg 1
Germany

The Bethe Salpeter Equation and the Relativistic Quark Model

Tamara S. Eisenschitz [+]

Deutsches Elektronen-Synchrotron DESY, Hamburg, Germany [*]

The SU(6) symmetry breaking inherent in relativistic quark models is described by using a solution of the Bethe Salpeter equation including spin Wigner rotations. Electroproduction matrix elements are calculated and effects of changing the parameters investigated.

[+] Most of this work submitted as part of the requirements for a PhD at Edinburgh University, Scotland.

[*] Royal Society European Fellow

1. Introduction

The non-relativistic potential quark model as developed by Copley, Karl and Obryk (CKO) and others [1] has provided quite a good description of resonance interactions and classification.

In resonance photoproduction off nucleons, it has been observed that the helicity 1/2 amplitudes of the $D_{13}(1520)$ and $F_{15}(1688)$ are small, possibly zero (see Walker in reference 1). In the CKO model there are two terms corresponding to spin and orbital angular momentum flip and for these two amplitudes they appear with opposite signs. One amplitude can be set to zero by adjusting the one free parameter to give complete cancellation. For an harmonic oscillator potential this parameter is the spring constant $\alpha^2 = m_q \omega$ (the other parameter, quark anomalous moment g is taken to be unity). Then the other amplitude turns out to be very small too.

However an harmonic oscillator potential leads to Gaussian wavefunctions which are undesirable in principle because of having the wrong analytic structure. Also electroproduction amplitudes change with stronger dependence on momentum transfer squared (q^2) than they should. So the CKO model is not as good in electroproduction as in photoproduction and the form factors need improving.

Another problem is that SU(6) is taken as an exact symmetry of the model. The SU(3) subgroup classifies the hadrons into multiplets and is a success, but when applied to interactions, SU(6) symmetry predictions are often wrong. Vertices are better described using current algebra.

It is thus desirable to improve the dynamics of the CKO model to improve form factors and describe the SU(6) symmetry breaking. We use the solution of the Bethe-Salpeter (BS) equation developed by Kellett for a relativistic model [2].

The main attraction of Kellett's model is that it explicitly Wigner rotates the spins of all three quarks even though the photon is assumed to interact with only one quark. This means that even though harmonic oscillator forces between the quarks are assumed, the wavefunctions will not be Gaussian. Lipes already showed in a much simpler model [3] that including the spin Wigner rotations and Lorentz contraction of the wavefunctions leads to correct dipole behaviour of the electromagnetic form factors.

One of the earliest attempts to create a relativistic quark model, due to Feynman Kislinger and Ravndal (FKR) [4] rewrote all CKO's three vectors as four vectors. However there is now a problem with unitarity. Having four dimensional excitations instead of three leads to states of imaginary mass which can only be eradicated by banning time-like excitations. This destroys unitarity since all excitations are needed to form a complete set of states. Lorentz covariance is also lost by singling out one direction as time.

Kellett solves the BS equation in the ladder approximation with an instantaneous interaction using the method of Brodsky and Primack [5] generalized to three quarks and strong binding.

The instantaneous interaction in all frames destroys Lorentz covariance in order to suppress the timelike excitations and is just as ad hoc as previous attempts. This is a general problem of relativistic quark models and remains unsolved here.

A brief description of the solution follows in section 2. Two solutions are presented, one with the interaction to second order in masses and the other with the full interaction. Comparison of the two shows how careful one must be making approximations in models where the (possibly effective) quark mass is small.

In section 3 we apply the model to N^* resonance electroproduction off nucleons, in particular the $D_{13}(1520)$, $F_{15}(1688)$ and $S_{11}(1535)$. We calculate helicity amplitudes and cross-sections for second order and full interactions and for the full interaction we investigate the range of variation of free parameters compatible with experiment.

For the full interaction, cross-sections are slightly larger than in the CKO model at small q^2 and seem to be in better agreement with the data. We see the improved q^2 dependence of the form factors in the shape of the cross-section curve.

However the magnitude of the cross-section is very sensitive to the precise value of α^2, the oscillator spring constant, so that one is not free to vary α^2 much. Although we could also vary g, the quark anomalous magnetic moment, it was only possible to make the helicity 1/2 photoproduction amplitude small for the F_{15}, not for the D_{13}. So this success of the CKO model is lost because of the need for the total cross-section to also

have the correct order of magnitude.

Finally we have a summary, section 4.

2. Solution

The BS equation [6] is a covariant generalization of the two body Schrödinger equation for dealing with bound state problems in relativistic quantum mechanics. In practice it can only be treated in the ladder approximation. Salpeter [7] rewrote the equation for the case of instantaneous interactions in the ladder approximation and Brodsky and Primack [5] generalized it to include the effect of an external field. Brodsky and Primack then solved this equation for weakly bound two fermion systems.
The generalization to three particles is straight forward [2], but to generalize to strong binding requires the assumption that the composite wavefunction in its rest frame has the form of a product of free quark spinors.

A trial solution for this wavefunction

$$\phi(p,q) = \left(\omega_a'\right) \otimes \left(\omega_b'\right) \otimes \left(\omega_c'\right) \phi_M \chi_S$$

is substituted into the Brodsky and Primack equation.

ω' and ω are 2 x 2 matrix functions of the relative momenta p and q and of $\underset{\sim}{\sigma}^{a,b,c}$, ϕ_M and χ_S are the usual [1] nonrelativistic spatial and SU(6) wavefunctions. For the spatial part, harmonic oscillator forces are assumed and ϕ_M will be the same wavefunctions as in the CKO and similar models.

For instance, the proton is in the ground state $(1s)^3$ completely symmetric state

$$\phi_M = \left(\frac{2\sqrt{3}}{\pi\alpha^2}\right)^{3/2} \exp\left[\frac{-1}{2\alpha^2}(3\underset{\sim}{p}^2 + 4\underset{\sim}{q}^2)\right]$$

Higher resonances are excited orbital states of the harmonic oscillator. The D_{13} is $(1s)^2(1p)$ etc. The corresponding SU(6) classifications are well known.

Solving for the spinors $\omega_{a,b,c}$, the CM wavefunction becomes

$$\phi = \int \frac{d^3\underset{\sim}{p}\; d^3\underset{\sim}{q}}{(2\pi)^3} N(\underset{\sim}{p},\underset{\sim}{q}) \begin{pmatrix} 1 \\ -\frac{\underset{\sim}{\sigma}^a \cdot \underset{\sim}{p}}{E_a + m_q} \end{pmatrix} \otimes \begin{pmatrix} 1 \\ \frac{\underset{\sim}{\sigma}^b \cdot (\frac{1}{2}\underset{\sim}{p} - \underset{\sim}{q})}{E_b + m_q} \end{pmatrix}$$

$$\otimes \begin{pmatrix} 1 \\ \frac{\underset{\sim}{\sigma}^c \cdot (\frac{1}{2}\underset{\sim}{p} + \underset{\sim}{q})}{E_c + m_q} \end{pmatrix} \phi_M \chi_s e^{i(\underset{\sim}{p}\cdot\underset{\sim}{x} + \underset{\sim}{q}\cdot\underset{\sim}{y}) - iMx_0}$$

$\omega_{a,b,c}$ represent relativistic corrections to the non-relativistic spin states χ . They exhibit Wigner rotations when Lorentz transformed.

Spinors are then

$$\begin{pmatrix} 1 - \frac{\underset{\sim}{\sigma}^a \cdot \underset{\sim}{P}}{E+M} \cdot \frac{\underset{\sim}{\sigma}^a \cdot \underset{\sim}{p}}{E_a + m_q} \\ \frac{\underset{\sim}{\sigma}^a \cdot \underset{\sim}{P}}{E+M} - \frac{\underset{\sim}{\sigma}^a \cdot \underset{\sim}{p}}{E_a + m_q} \end{pmatrix}$$

with $\underset{\sim}{P}$ the centre of mass momentum.

The normalization

$$N(p,q) = \left[\frac{E_a + m_q}{2E_a} \cdot \frac{E_b + m_q}{2E_b} \cdot \frac{E_c + m_q}{2E_c} \right]^{1/2}$$

With $E_{a,b,c}$ effective quark energies: $E_a = (p^2 + m_q^2)^{1/2}$ etc.

The general wavefunction in an arbitrary frame is found by Lorentz boosting this rest frame wavefunction.

Since the wavefunction is a product of nonrelativistic parts and spinors, the general matrix element can be written in terms of an effective Hamiltonian (for interaction of quark a) $H^a(p,q)$ between nonrelativistic wavefunctions $|A\rangle$, $|B\rangle$:

$$3\int d^3p \; d^3q \; \langle B | H^a(p\,q) | A \rangle$$

It is multiplied by 3 to account for all the quarks. H^a is a product of spinors, projection operators and the appropriate part of the quark current. Note that for the interaction on a, the spins of b and c still must enter because they are not truly spectators being Wigner rotated in the course of the interaction.

Exact SU(6) symmetry is assumed for the three quarks so that they have the same mass, magnetic moment etc.

$$H^a(p,q) = \left(\frac{E_B + m_B}{2m_B}\right)^{3/2} N(p\,q)\, N(\tilde{p} + \tfrac{2}{3}k, \tilde{q})$$
$$\cdot (1 + \rho_a s_a, s_a + \rho_a)\, \Lambda_+^a (\tfrac{1}{2}k - \tilde{p})\, \gamma_0^a J_\mu^a\, \epsilon^\mu \begin{pmatrix} 1 \\ \eta_a \end{pmatrix}$$
$$\cdot (1 + \rho_b s_b, s_b + \rho_b) \begin{pmatrix} 1 \\ \eta_b \end{pmatrix}$$
$$\cdot (1 + \rho_c s_c, s_c + \rho_c) \begin{pmatrix} 1 \\ \eta_c \end{pmatrix}$$

where λ_i = SU(3) matrices

$\Lambda_+^a(p_a)$ = free quark projection operator

$k = p' - p$

ϵ_μ = photon polarization 4 vector

$$J_\mu = \bar{\psi}(p') \left[\gamma_\mu + \frac{K}{2m_q}\, i\, \sigma_{\mu\nu} k^\nu\right] \frac{\lambda_i}{2} \psi(p)$$

K = anomalous magnetic moment, $g = 1 + K$

$$s_i = \frac{\sigma^i \cdot P}{E_B + m_B}$$

$$\rho_a = -\frac{\sigma^a \cdot k}{E_a + m_q} \qquad \rho_b = \frac{\sigma^b \cdot (\frac{1}{2}P - q)}{E_b + m_q}$$

$$\rho_c = \frac{\sigma^c \cdot (\frac{1}{2}P + q)}{E_c + m_q}$$

with the η_i obtained from the ρ_i by $p \to \tilde{p} + \frac{2}{3}k$ and $q \to \tilde{q}$. P is the centre of mass momentum and $\tilde{p}$, $\tilde{q}$ are quark relative momenta for the Lorentz contracted wavefunction. For more details of the solution see Kellett ref. (2).

3. Application to Resonance Electroproduction

a. Second order amplitudes

The Hamiltonian can be expanded in a $1/m$ series where the masses may be either quark or nucleon and resonance masses. The first order is just the CKO Hamiltonian

$$H^a = \frac{\underset{\sim}{p} \cdot \underset{\sim}{\epsilon}}{m_q} + i \frac{\underset{\sim}{\sigma}^a \cdot \underset{\sim}{\epsilon} \times \underset{\sim}{k}}{2 m_q}$$

(assuming anomalous moment g = 1 throughout this section).

Going to second order gives the relativistic corrections to the CKO model. The terms are not very informative and the transverse ones can be seen in reference 2. We used them to calculate the helicity amplitudes for $D_{13}(1520)$ and $F_{15}(1688)$ electroproduction off nucleons.

Setting the helicity 1/2 amplitude of the F_{15} to zero determines the value of α^2 the oscillator spring constant just as in the non-relativistic case. With $m_q = 0.33$ GeV we have $\alpha^2 = 0.328$ GeV^2. Kellett used $\alpha^2 = 0.35$ given by the slope of Regge trajectories in FKR [4], but since the argument requires heavy quarks it is not applicable here. Once these parameters have been fixed there is no more arbitraryness. One then calculates numbers.

Now we may calculate the D_{13} transverse and longitudinal cross-sections and the ratio $R = A_{1/2}/A_{3/2}$. These are drawn in figures 1, 2 and 3 and

are to be compared with the predictions of the CKO model drawn alongside.

We note particularly that R rises fairly gently in this model in contrast to the very rapid change from CKO characteristic of their Gaussian form factors. This flattening is due to the inclusion of the Lorentz contraction of the wavefunction and the Wigner rotation of all the spins as already discussed.

The cross-sections have similar q^2 dependence to those of the CKO model but their magnitudes are rather smaller and do not agree with experiment. In figure 4 we have data for the second resonance region [8] which is predominantly D_{13} (the upper points are the complete peak, the lower ones are the S_{11}). This is not a direct comparison: σ_t and σ_l are not separated and the S_{11} accounts for 20 to 30 μb, but even then the graphs for the second order are rather too low.

All the calculations are in the isobar rest frame but according to Kellett [9] frame dependence is quite small, so we will not bother about it.

Calculations are not carried beyond $q^2 = -1$. The CKO model is explicitly non-relativistic and in Kellett's model the approximation of instantaneous interaction in all frames breaks down. Also a crude harmonic oscillator potential is unlikely to be even approximately correct in a highly relativistic domain.

b. The full integral

Because the $1/m$ expansion above involved the small quark mass of 0.33 GeV it cannot be convergent and is therefore unreliable. We want to compare it with the full integral. The general matrix element is written out in detail. The spin matrix elements are calculated by hand but the spatial integrals have to be done numerically.

Using m_q = 0.33 GeV, g = 1 and α^2 = 0.35 GeV^2 we calculate σ_t, σ_l and R as before for the D_{13}. They are drawn in figures 1, 2 and 3. We see quite noticeable differences from the second order graphs and from CKO.

In figure 5 we now compare the data for just the D_{13} with the total cross-sections of the CKO and Kellett models. The data is taken by just subtracting the S_{11} points from the total peak in figure 4. Therefore points may still be too high owing to contributions from other resonances. Since there are only two main second peak resonances, this should be a very small error.

For the theoretical cross-sections $\sigma_T = \sigma_t + \epsilon \sigma_l$ where we calculated σ_t and σ_l . We took ϵ = 1 since in these experiments the photons are not polarized and ϵ is 1 or very close to it. ϵ = 1 is the largest possible value so that σ_T are at their maxima.

We see that the curve for the full integral follows the shape of the data very well, better than the other two. It is only a little low.

In figure 3 we can compare the calculated ratios of helicity amplitudes

with the data. The data is obtained from an analysis by Devenish and Lyth [10]. There is a spread of possibilities due to uncertainty in parameterizing the resonances in their fits. The constraint of requiring smooth curves makes it very unlikely that the true values lie outside the shaded region.

We see that it is the second order of Kellett's model which gives the most reasonable slope. The CKO ratio changes far too steeply. The full integral leads to a ratio which is almost flat and far too high. The reason for this is the following:

The two helicity amplitudes for photoexcitation of the D_{13} are

$$A_{\frac{1}{2}} \approx \sqrt{\tfrac{3}{2}}\, R_{10} - \tfrac{\sqrt{3}}{2}\, R_{11}$$

$$A_{3/2} \approx \tfrac{3}{2}\, R_{11}$$

where R_{10} and R_{11} are spin and orbital flip matrix elements respectively. In this model it turns out that R_{10} is almost negligible compared to R_{11} so that

$$\frac{A_{1/2}}{A_{3/2}} \approx \frac{\sqrt{3}}{3} = 0.57$$

for all q^2 and any values of the free parameters. So the ratio cannot be improved in any way here.

The smallness of the helicity 1/2 amplitude in photoproduction, which in the CKO model comes about through cancellation between the R_{10} and R_{11},

must here come from the overall normalization.

None of the three theoretical curves gives much of a fit to the ratio and this is still an unsolved problem for quark models.

Returning to the full integral, we need to check on the effectiveness of the choice of α^2 in keeping the helicity 1/2 amplitude small for the D_{13} and F_{15}. For this we calculate the backward differential cross-section for photoproduction where only the $A_{1/2}$ contributes.

$$\frac{d\sigma}{d\Omega}\Big|_{\theta=\pi} \approx |A_{\frac{1}{2}}|^2$$

For the D_{13} $\quad \frac{d\sigma}{d\Omega}\Big|_{\theta=\pi} = 0.62\ \mu b.\ sr^{-1}$

F_{15} $\quad = 0.074\ \mu b.\ sr^{-1}$

compared with 0.08 and 0.01 $\mu b\ sr^{-1}$ respectively experimentally [1,11]. This is not a very good agreement. So we must try and adjust the free parameters of the model to improve the fit.

It must be noted that since only a change in normalization will improve $\frac{d\sigma}{d\Omega}$, we have little scope to vary α^2 without spoiling the good agreement of $\sigma_T = \int d\Omega \ \frac{d\sigma}{d\Omega}$

We can vary α^2 and also g. Taking $\alpha^2 = 0.35$, 0.5, 0.75 and 1 and varying g between 1 and 10 we computed many values of the differential cross-section for the D_{13} and F_{15}. The quark mass was changed with g according to

$$\mu = \frac{eg}{2m_q}$$

although this is arbitrary since in a strong binding situation the binding may also affect the mass. Plotting g vs $\frac{d\sigma}{d\Omega}$ at fixed α^2 and α^2 vs $\frac{d\sigma}{d\Omega}$ at fixed g and extrapolating, values of g and α^2 were found for which $\frac{d\sigma}{d\Omega}$ was 0.08 for the D_{13} and 0.01 for the F_{15}. Graphs were plotted of these values, figure 6. They are double valued, going between the curves corresponds to a larger differential cross-section.

We see in figure 6 that the D_{13} and F_{15} curves have the same values at quite a number of points. However, we are really only interested in values of α^2 close to 0.35 because of the normalization of the total cross-section. (For instance σ_t = 0.17 μb at $q^2 = 0$ when $\alpha^2 = 1$ and g = 1). This sensitivity is mainly due to a factor of $\alpha^{-11/2}$ in the amplitudes. In the region of $\alpha^2 = 0.35$ we have only drawn the curve for the F_{15}. The F_{15} amplitude agrees with experiment at $\alpha^2 = 0.35$, g = 0.95. The extrapolations for the D_{13} are not valid in this region. There is a large discontinuity between g = 1 and g = 2. If large g values are extrapolated, one would have $\frac{d\sigma}{d\Omega}\Big|_{\theta=\pi} = 0.01\ \mu b.sr^{-1}$ at g = 1 instead of the 0.62 calculated. The reason for this big difference is that the introduction of the anomalous moment part of the current must have a large effect (although it does not have such an effect for the F_{15}). A consequence of this discontinuity is that around $\alpha^2 = 0.35$ there is no value of g for which the differential cross-section acquires its experimental value.

The conclusion here is that the parameters can be fitted to give good values and shape for the total electroproduction cross-section and the experimental value for the differential photoproduction cross-section of the F_{15} only. The differential cross-section for the D_{13} will be about ten times too big and the ratio of helicity amplitudes is effectively a ratio of Clebsch-Gordan coefficients so there is no possibility of improving this fit.

c. The S_{11} (1535) resonance

There is one other resonance of particular interest, the $S_{11}(1535)$. According to new data presented at the Bonn conference [8], the total cross-section for electroproduction of the S_{11} is constant with q^2. The CKO model [1] predicts a fall just as for the D_{13} (figure 7). From the calculations discussed here using the full integral, Kellett's model also predicts a sharp fall with or without an anomalous moment. The spin and orbital flip matrix elements are the same as for the D_{13} only combined with different Clebsch-Gordan coefficients. It is the dominance of the orbital flip part which causes the steep fall for the S_{11} just as it makes the ratio of helicity amplitudes for the D_{13} flat. The solution of the one problem may perhaps help the other.

This is a definite failure of the model inherent in its structure.

However another possible way out for the S_{11} is to consider mixing. The curves of figure 7 are arrived at by treating the $S_{11}(1535)$ as a member of the $L^P = 1^-$ octet with quark spin 1/2. There is an $S_{11}(1700)$

with quark spin 3/2 in the same octet and there could be mixing.

Then

$$S_{11}(1535) = (8^{1/2}) \cos\theta - (8^{3/2}) \sin\theta$$

This was already considered by CKO who needed $\theta = 70^{\circ}$ to correct their photoproduction value. For the Kellett model the discrepancy is less. Unfortunately the pure quark spin 3/2 state does not couple to the electromagnetic current at all (for electroproduction off a proton) as was first pointed out by Moorhouse [12], so the only effect of the mixing is to multiply the previous amplitudes by $\cos\theta$. This reduces the overall normalization but cannot affect the shape of the curve. So the prediction would still be a falling cross-section rather than a flat one and the discrepancy still stands. One encouraging sign: The angle required to correct the photoproduction value is 48°. From strong interactions [13] ($S_{11} \rightarrow N\eta$) an angle of 45° is indicated. These are in good agreement.

The $S_{11}(1700)$ will now have a nonzero coupling to the electromagnetic current. Using $\theta = 48^{\circ}$ we can calculate this amplitude which will be

$$S_{11}(1700) = (8^{1/2}) \sin\theta + (8^{3/2}) \cos\theta$$

$$= (8^{1/2}) \sin\theta$$

$$= 0.24 \text{ GeV}^{-1/2}$$

to be compared with an upper limit of $0.11 \text{ GeV}^{-1/2}$ from Moorhouse and

Oberlack[11] (but only 0.05 $GeV^{-1/2}$ from Devenish et al. [14]). The calculated number is a little large but not unreasonable.

4. Summary

The model has two main achievements.

A. Despite the harmonic oscillator potential, the form factors are not Gaussian. This is due to including the Lorentz contraction of the wave-functions and the spin Wigner rotations. We see in figure 5 that the shape of the total cross-section curve fits the data much better than that of the CKO model.

B. The cross-sections for the D_{13} resonance appear to be in better agreement with the data when we take the full integral in Kellett's model than in CKO.

There are still problems

1. The instantaneous interaction
2. The expansion in inverse masses. Does one believe the expansion or only the full integral? The first order of the expansion is CKO which has been a quite successful model, so the second order should also have some significance although it is very different from the full integral.
3. The dominance of the orbital flip over spin flip terms in the helicity 1/2 amplitude of the D_{13}. This problem must be solved in order to make any further progress. It has three consequences:

a. The ratio of helicity amplitudes is essentially constant, depending on just Clebsch-Gordan coefficients.

b. The photoproduction helicity 1/2 amplitude of the D_{13} cannot be made small simultaneously with that of the F_{15} without destroying the order of magnitude agreement of the D_{13} total cross-section.

c. The electroproduction cross-section for the S_{11} falls steeply with q^2 instead of remaining flat.

Finally, the introduction of a realistic spin treatment is a step forward but the involved interaction thus produced reduces the degree of agreement with experiment obtained in naive models.

Acknowledgements

I particularly thank Dr. K.C. Bowler for all his help and encouragement during the course of this research.

I also thank Dr. B.H. Kellett for detailed discussions of his work and Dr. J.W. Searl for advice on the computing.

I am very grateful to Dr. M. Krammer and Dr. D. Schildknecht for reading the manuscript and discussing the results.

Finally I acknowledge the receipt of an SRC research training grant.

References

1. D. Faiman and A.W. Hendry, Phys. Rev. 173, (1968) 1720
180, (1969) 1572
L.A. Copley, G. Karl and E. Obryk, Phys. Letters 29B, (1969) 117
Nucl. Phys. B13, (1969) 303
K.C. Bowler, Phys. Rev. D1, (1970) 926
N. Thornber, Phys. Rev. 169, (1968) 1096
173, (1968) 1414
D3, (1971) 787
R.L. Walker, Proceedings of the 4th International Symposium on Electron and Photon Interactions at High Energies, Liverpool 1969, Ed. D.W. Braben, (Daresbury 1969)

2. B.H. Kellett, Ann. Phys. 87, (1974) 60
Phys. Rev. D10, (1974) 2269

3. R.G. Lipes, Phys. Rev. D5, (1972) 2849

4. R.P. Feynman, M. Kislinger and F. Ravndal, Phys. Rev. D3, (1971) 2706

5. S.J. Brodsky and J.R. Primack, Ann. Phys. 52, (1969) 315

6. E.E. Salpeter and H.A. Bethe, Phys. Rev. 84, (1951) 1232

7. E.E. Salpeter, Phys. Rev. 87, (1952) 328

8. A.B. Clegg, Proceedings of the 6th International Symposium on Electron and Photon Interactions at High Energies, Bonn 1973, Ed. H. Rollnik and W. Pfeil (North Holland 1974)

9. Private communication

10. R.C.E. Devenish and D.H. Lyth, DESY report No. 75/4

11. R.G. Moorhouse and H. Oberlack, Phys. Letters 43B, (1973) 44

12. R.G. Moorhouse, Phys. Rev. Letters 16, (1966) 772

13. W.P. Petersen and J.L. Rosner, Phys. Rev. D6, (1972) 820
D. Faiman and D.E. Plane, Phys. Letters 39B, (1972) 358
Nucl. Phys. B50, (1972) 379

14. R.C.E. Devenish, D.H. Lyth and W.A. Rankin, Phys. Letters 52B, (1974) 227

Figure Captions

1. Predictions of the CKO [1] and Kellett [2] models for the transverse electroproduction cross-section of the D_{13}.

2. Predictions for the D_{13} longitudinal cross-section.

3. Predictions for the ratio of helicity amplitudes in the D_{13} compared with data from ref. 10.

4. Data for the second resonance region from Clegg ref. 8. The upper points are for the full peak, the lower points for the $S_{11}(1535)$ only.

5. Data points for the D_{13} only, extracted from fig. 4 and compared with predicted total cross-sections taken from figs. 1 and 2.

6. Predictions for the values of the parameters α^2 and g required in the full Kellett model to give the correct differential cross-section for photoproduction of the D_{13} and F_{15}.

7. Predicted transverse and longitudinal cross-sections for the S_{11}.

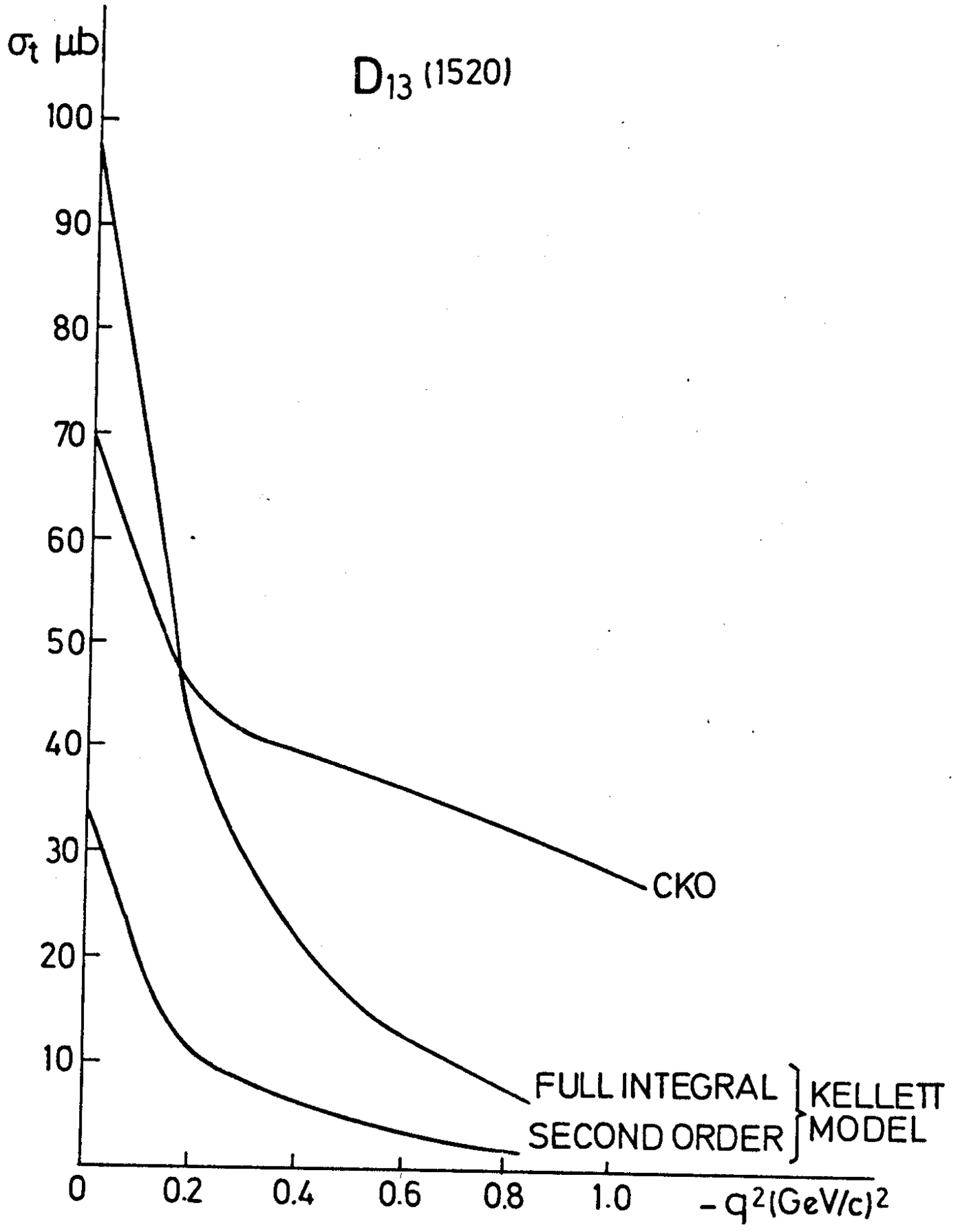
σ_t μb
D_{13} (1520)
100
90
80
70
60
50
40
30
20
10
CKO
FULL INTEGRAL
SECOND ORDER
KELLETT MODEL
0
0.2
0.4
0.6
0.8
1.0
$-q^2$(GeV/c)^2

FIG. 1

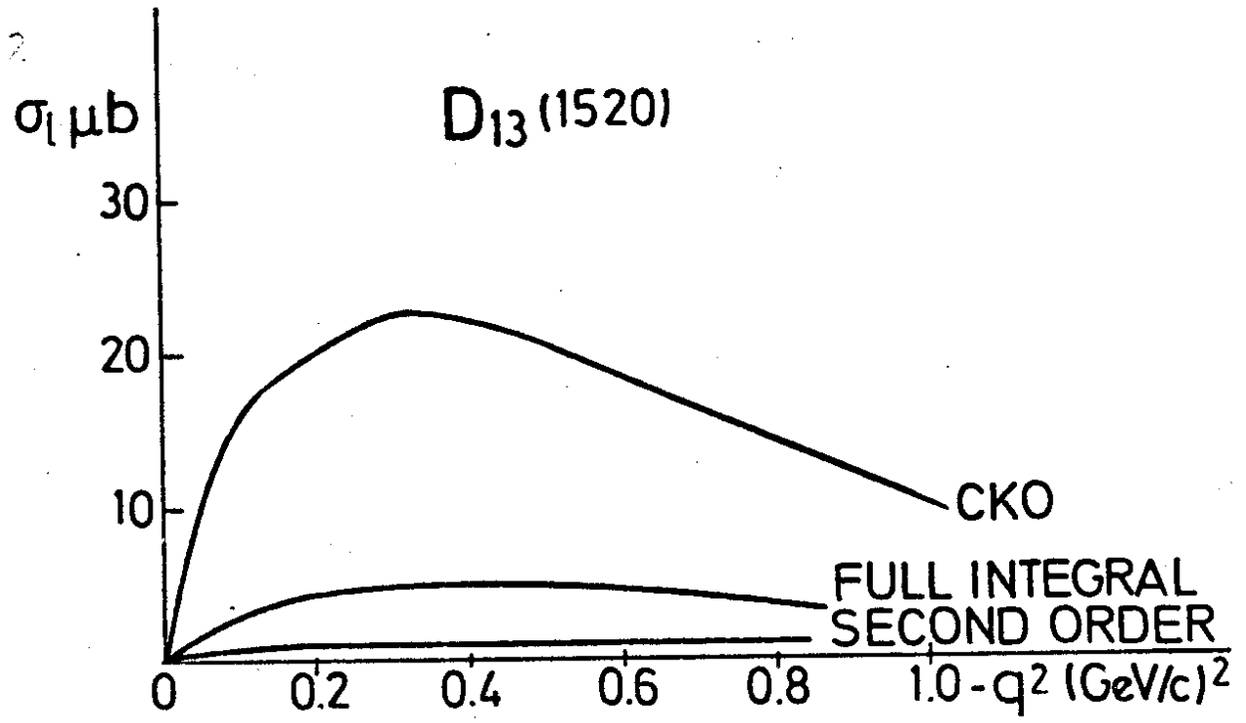
σ_l μb
D_{13}(1520)
30
20
10
CKO
FULL INTEGRAL
SECOND ORDER
0
0.2
0.4
0.6
0.8
1.0 - q^2 (GeV/c)^2

FIG. 2

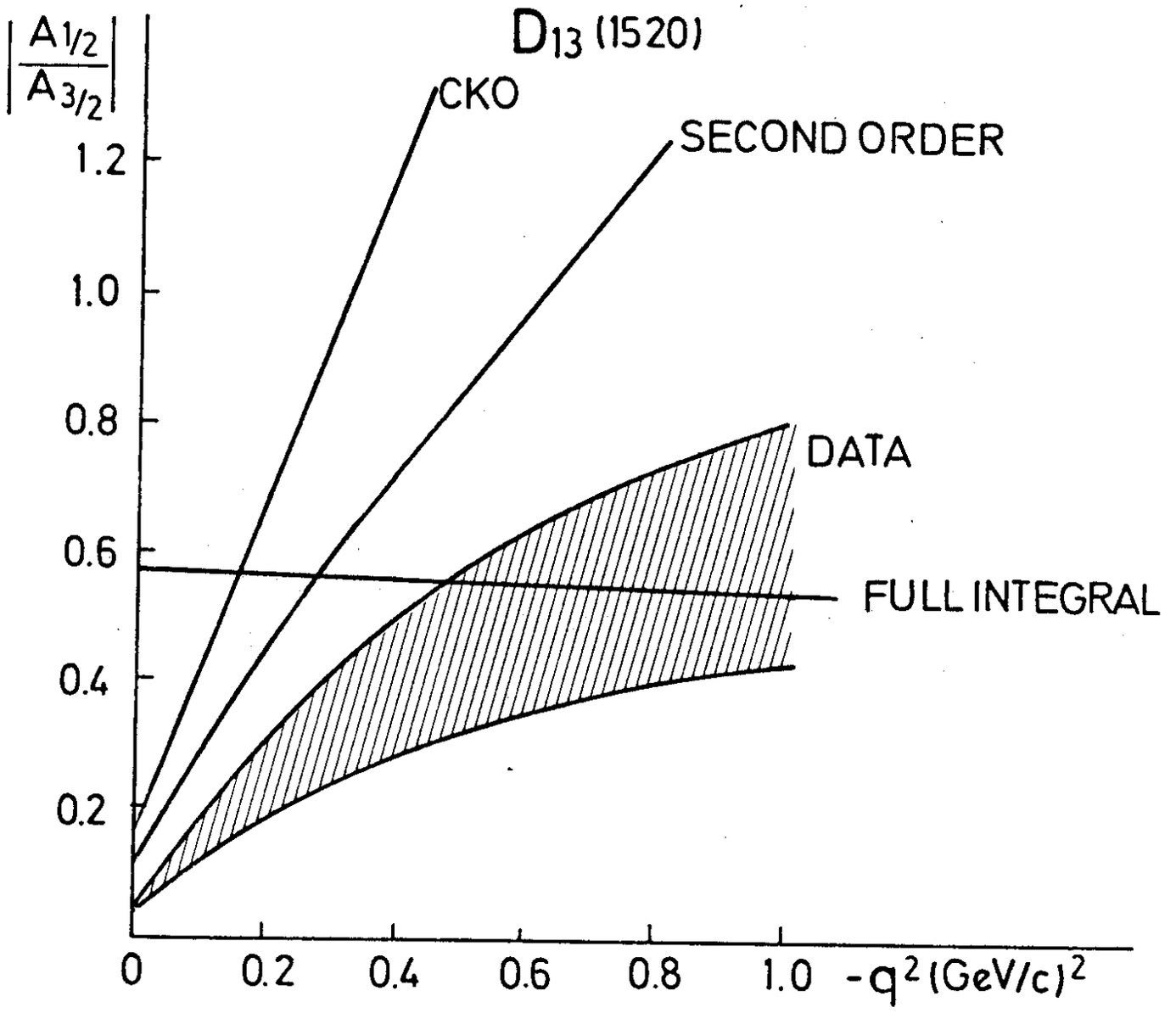
D_{13} (1520)
$\left|\frac{A_{1/2}}{A_{3/2}}\right|$
CKO
SECOND ORDER
DATA
FULL INTEGRAL
1.2
1.0
0.8
0.6
0.4
0.2
0
0.2
0.4
0.6
0.8
1.0
$-q^2$ (GeV/c)^2

FIG. 3

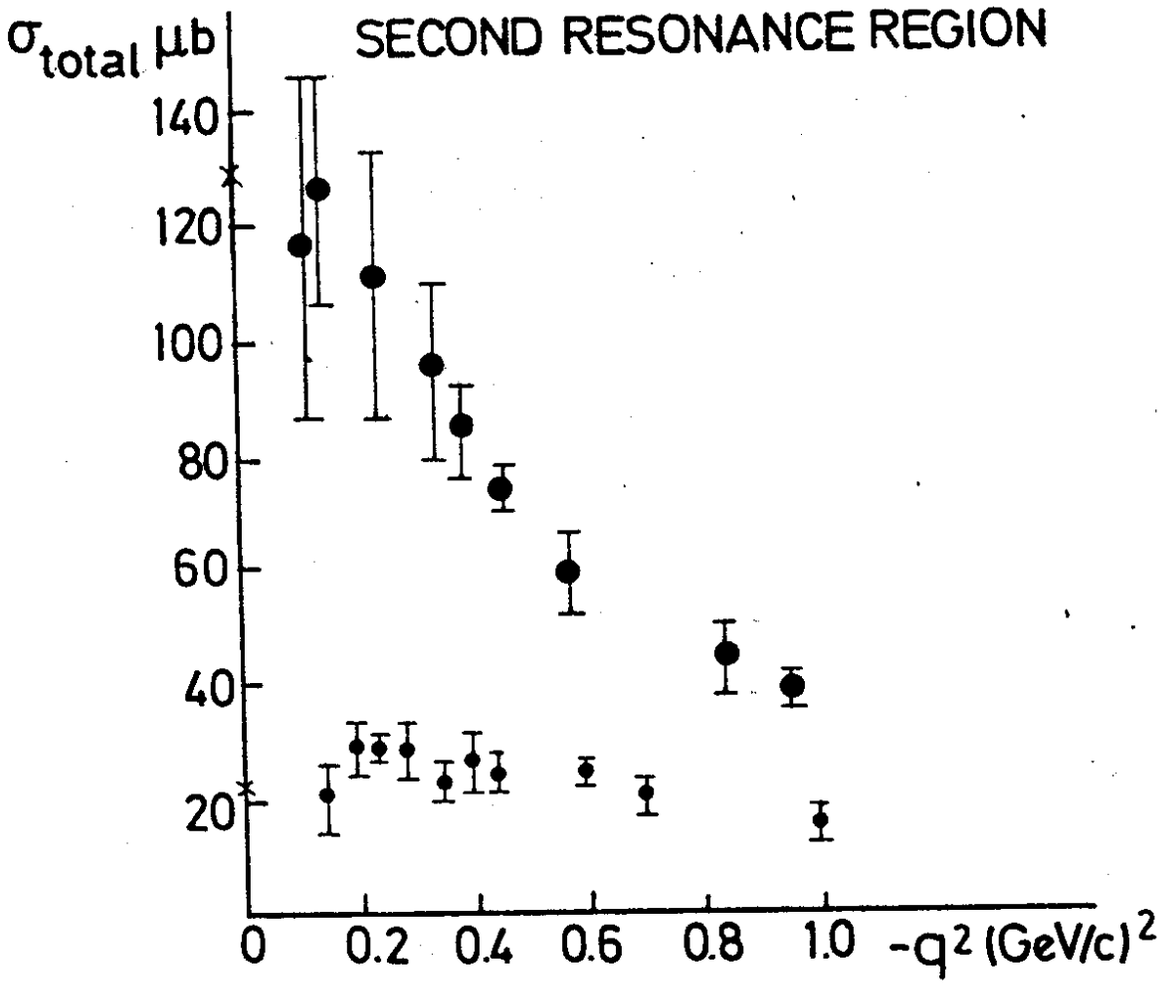
σ_{total} μb
SECOND RESONANCE REGION
140
120
100
80
60
40
20
0
0.2
0.4
0.6
0.8
1.0
$-q^2$ (GeV/c)^2

FIG. 4

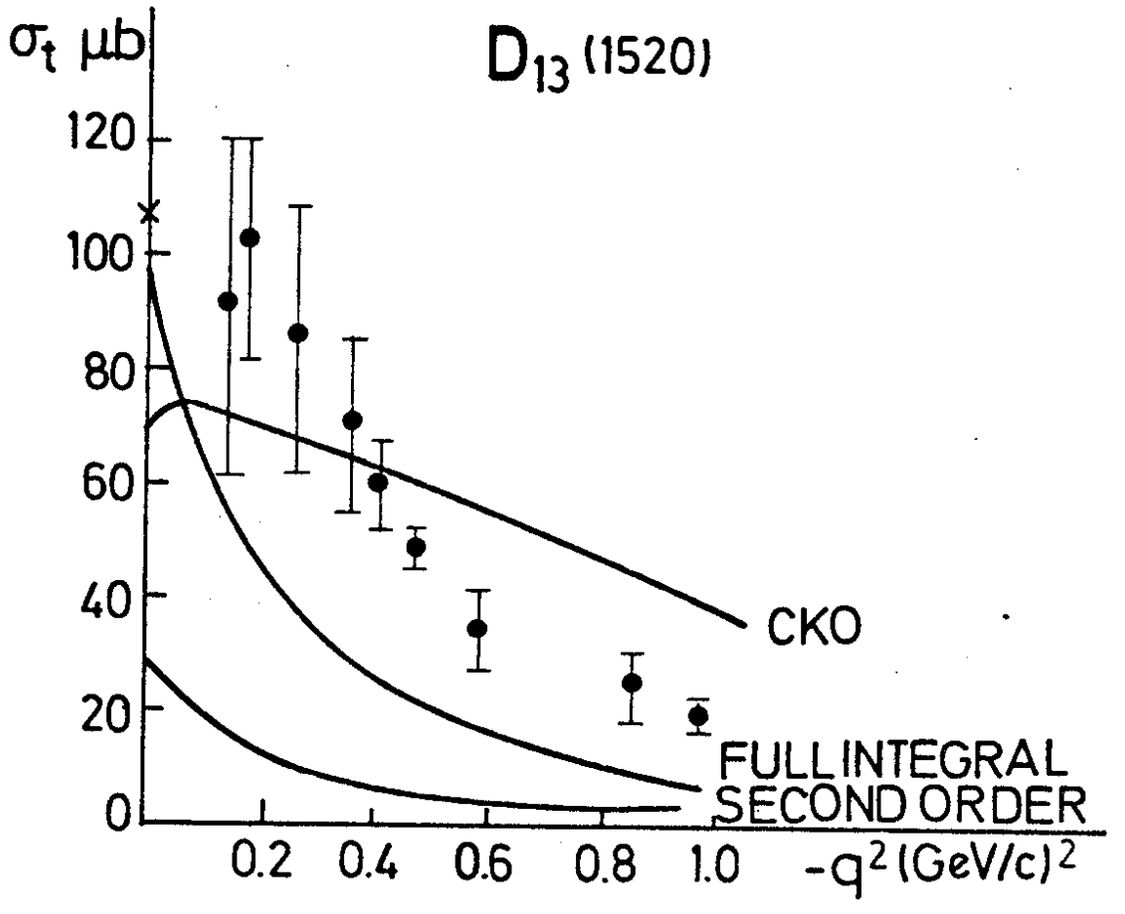
σ_t μb
D_{13} (1520)
120
100
80
60
40
20
0
0.2
0.4
0.6
0.8
1.0
$-q^2$ (GeV/c)^2
CKO
FULL INTEGRAL
SECOND ORDER

FIG. 5

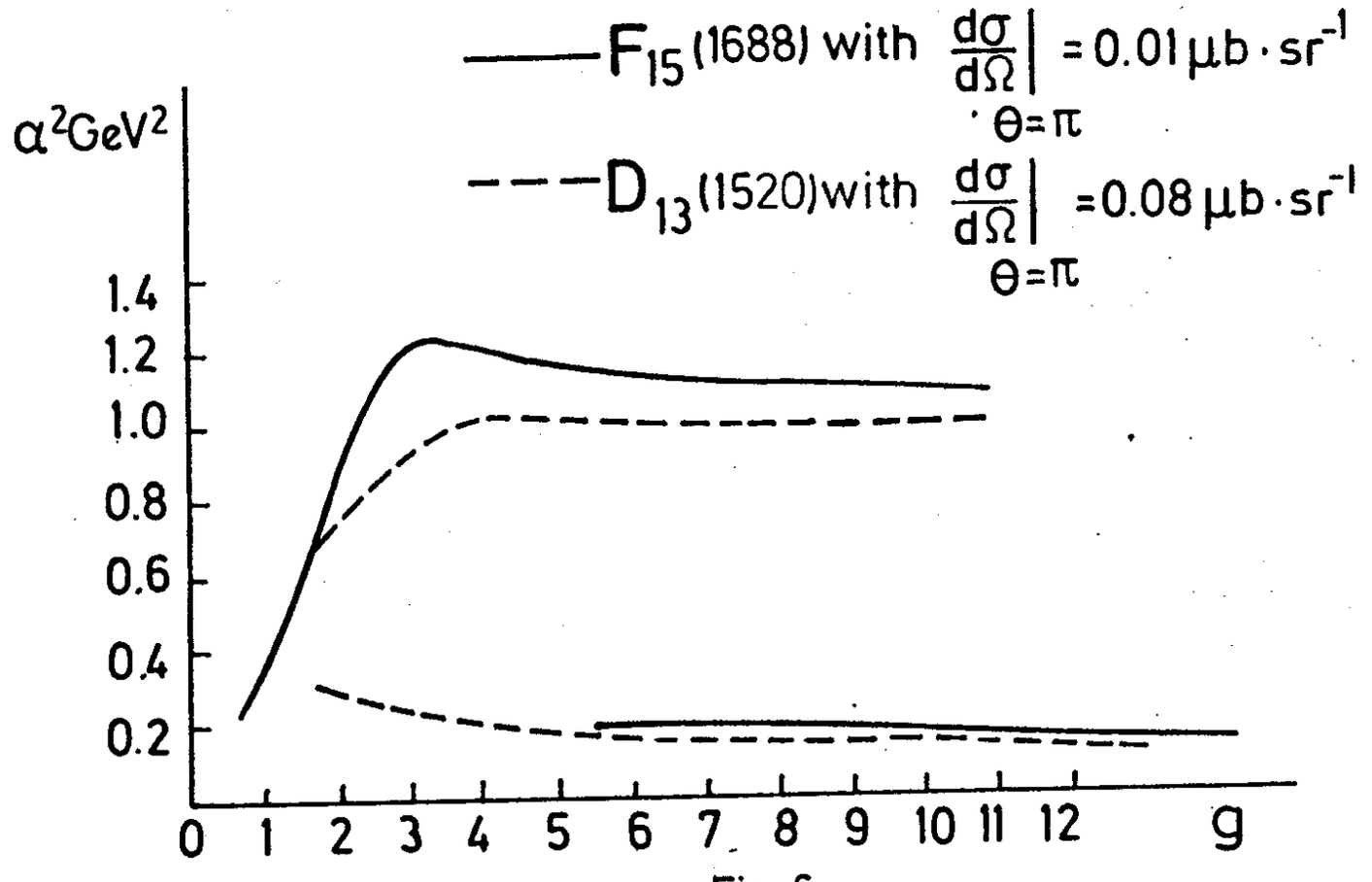
$F_{15}(1688)$ with $\frac{d\sigma}{d\Omega}\Big|_{\theta=\pi} = 0.01\,\mu b \cdot sr^{-1}$
$D_{13}(1520)$ with $\frac{d\sigma}{d\Omega}\Big|_{\theta=\pi} = 0.08\,\mu b \cdot sr^{-1}$
$\alpha^2 GeV^2$
1.4
1.2
1.0
0.8
0.6
0.4
0.2
0 1 2 3 4 5 6 7 8 9 10 11 12 g

Fig. 6

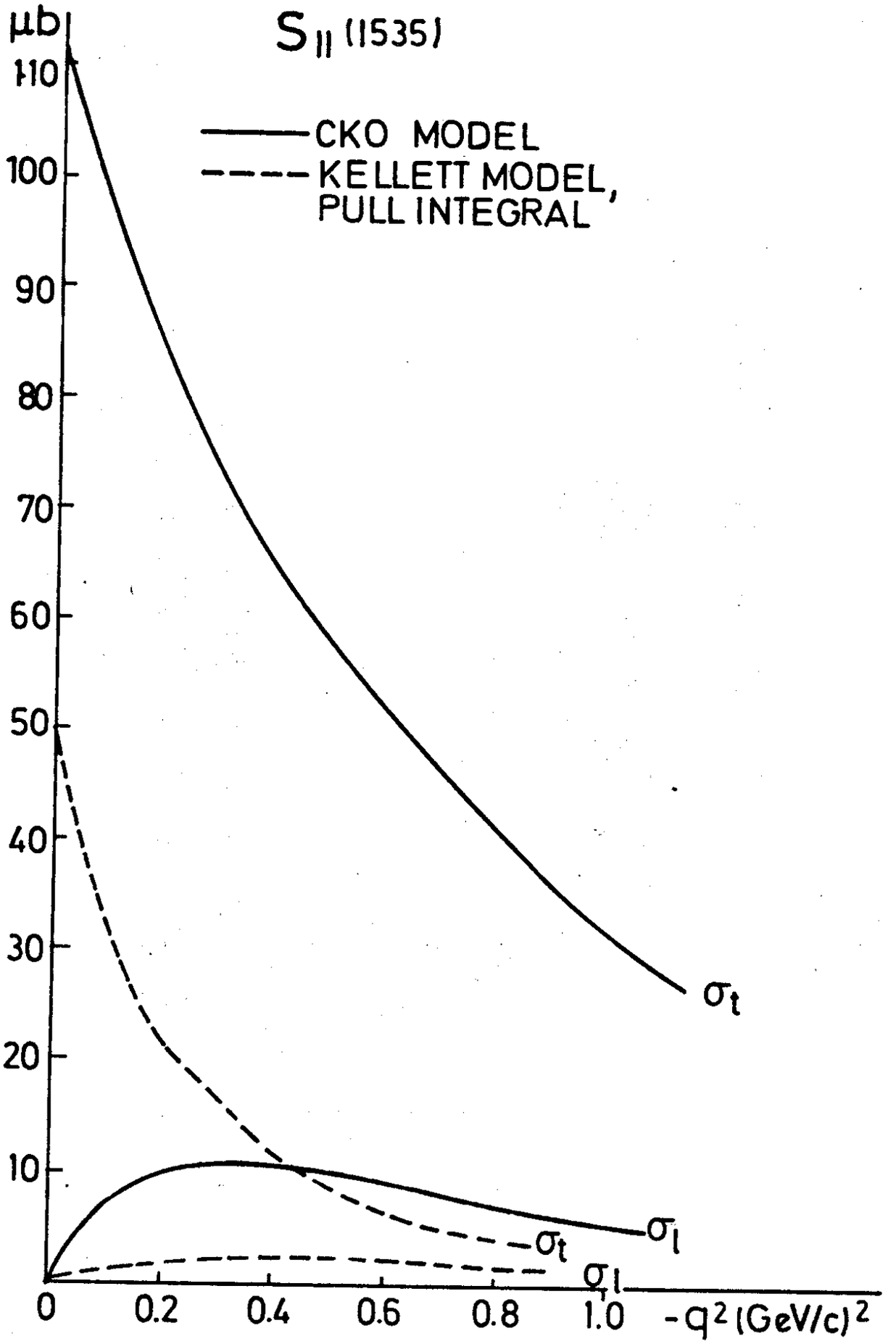
μb
S_{11} (1535)
110
100
90
80
70
60
50
40
30
20
10
CKO MODEL
KELLETT MODEL,
PULL INTEGRAL
σ_t
σ_l
σ_t
σ_l
0
0.2
0.4
0.6
0.8
1.0
$-q^2$ (GeV/c)^2

FIG. 7